

# Configurational entropy and Newton's Law in double sine-Gordon braneworlds

W. T. Cruz,<sup>1,\*</sup> D. M. Dantas,<sup>2,†</sup> R. V. Maluf,<sup>2,‡</sup> and C. A. S. Almeida<sup>2,§</sup>

<sup>1</sup>*Instituto Federal de Educação, Ciência e Tecnologia do Ceará (IFCE),  
Campus Juazeiro do Norte, 63040-000 Juazeiro do Norte - CE - Brazil*

<sup>2</sup>*Universidade Federal do Ceará (UFC),  
Departamento de Física, Campus do Pici,  
Fortaleza - CE, C.P. 6030, 60455-760 - Brazil*

(Dated: April 27, 2022)

## Abstract

In this work, we consider a five-dimensional thick brane scenario dynamically generated by a scalar field coupled to gravity. We evaluate the Shannon-like entropic measure to spatially-localized functions known as configurational entropy (CE) for a brane generated by a new double sine-Gordon (DSG) potential. The CE has been shown in several recent works a tool that selects critical points and brings out phase transitions in confined energy models with arbitrary parameters. We are interested in the DSG scenario because it represents a thick five-dimensional model where occur phase transitions on the scalar field solutions. The graviton resonance lifetimes are related to the existence of scales on which 4D gravity is recovered. As a result, we correlate the critical points defined by the CE with the phase transitions. At last, we calculate the corrections to the Newton's Law coming from the graviton modes.

PACS numbers:

---

\*Electronic address: wilami@ifce.edu.br

†Electronic address: davi@fisica.ufc.br

‡Electronic address: r.v.maluf@fisica.ufc.br

§Electronic address: carlos@fisica.ufc.br

## I. INTRODUCTION

The term Configuration Entropy (CE) was reintroduced by the Gleiser and Stamatopoulos in 2012 [1], on which it is based on Shannon's information theory [2]. In this view, the CE represents a measure of stability applied to the spatially-bounded energy system. To demonstrate the CE applicability, the early works [1, 3, 4] shows how this measure can be used to find stable Q -balls and the Chandrasekhar limit for white dwarfs [3]. Further, the CE was applied to investigate the nonequilibrium dynamics of spontaneous symmetry-breaking [4] and also to obtain bounds on the stability of various self-gravitating astrophysical objects [5]. Thereupon, several papers was released applying the CE in various areas of physics in the last years [6–10], as topics in AdS/QCD holography [6, 7], Kortewegde Vries equation [8], Bose-Einstein condensate [9] and predicting the atomic decay rates [10].

In the present paper, we focus on the recent application of CE to braneworlds models [11–16]. In fact, the CE was proved useful for determining stable parameter on brane models with a single scalar fields configuration, as the case of  $F(R)$  brane models [11], the Bloch brane [12], the Weyl's brane [13], the string-like models [14], braneworlds scenarios from deformed defect chains [15] and the (single) sine-Gordon model [16]. As another interesting feature, the CE also determines where phase transitions occur in the double-kinks models [12, 13], as the case of some degenerate branes [12]. On the other hand, the kink into multi-kinks phase transitions have some important applications. In general, multi-kink models tend to preserve stability where single-kinks models are no more stables [17], beside the multi-kinks have some specifics experimental applications [18, 19]. Moreover, in the braneworld context, multi-kinks models allow the appearance of multiple resonant states [20, 21].

This paper aims to explore the configuration of the double sine-Gordon model (DSG). The DSG model represents a version of the sine-Gordon model where the scalar fields is a double-kink, instead one single kink. We are especially interested in the DSG setup because it presents a smooth transition between the usual kink solution and the two-kink structure. In this work, we propose a new kind of the DSG potential that allows the convergence from the two-kinks DSG model to a single-kink model similar to the sine-Gordon (SG) scenario through the parameter  $a$ . From the previous works ([12]), we can observe that the phase transitions in brane solutions dynamically generated by scalar fields are predicted by the existence of a minimum on the Shannon-like entropic measure to the energy density. Since

the DSG model possesses a phase transition on the scalar field solution, we expect to obtain the same behavior to the CE measure, that is, a minimum on the CE related with the phase transition.

After mapping the DSG setup regarding the CE measure, we proceed to investigate the graviton localization. In our previous work [20], we have shown the existence of resonances on the massive spectrum of the graviton on the DSG setup. The existence of such resonances is related to the existence of a long-distance scale where the Newtonian potential is valid [22, 23]. Moreover, we calculate the corrections to Newton's potential in DSG and SG model and its correlations with the resonant modes. Additionally, the localization of fields as gravity [20] and the vector gauge-fields and the correction to the Coulomb's Laws [21] have been performed on a similar DSG model.

This work is organized as follows. In Sec. II we review the double sine-Gordon brane scenario where we show that the DSG model can be led to the simple sine-Gordon model according to the choice of parameters. In Sec. III, our first results are shown. We apply the CE method in order to obtain the critical points for the  $a$  parameter on DSG model. In Sec. IV, we detail the gravity localization on the DSG model in subsection IV A, the resonant modes in subsection IV B. The corrections to Newton's law on DSG model are computed in subsection IV C. Finally, we summarize our results and final comments in Sec. V.

## II. DOUBLE SINE-GORDON BRANES

To construct a braneworld based on the sine-Gordon (SG) potential, we first consider a scalar field coupled to gravity defined by the following action

$$S = \int d^5x \sqrt{-G} \left[ \frac{1}{4} R - \frac{1}{2} \partial_\mu \phi \partial^\mu \phi - V(\phi) \right]. \quad (1)$$

The scalar field depends only on the extra dimensional coordinate  $y$  on which the space-time is asymptotic  $AdS_5$  with the metric  $ds^2 = e^{2A(y)} \eta_{\mu\nu} dx^\mu dx^\nu + dy^2$ , where  $A(y)$  is the warp factor, and  $R$  is the scalar curvature. For the metric  $\eta_{\mu\nu}$  with  $\mu, \nu = 0, 1..3$ , we use the signature  $(-, +, +, +)$ .

The resulting equations of motion are

$$\phi'^2 - 2V(\phi) = 6A'^2 \quad (2)$$

$$\phi'^2 + 2V(\phi) = -6A'^2 - 3A'' \quad (3)$$

$$\phi'' + 4A'\phi' = \frac{\partial V}{\partial \phi}. \quad (4)$$

To transform the motion equations into a set of first-order equations, we write the choose the potential concerning a superpotential  $W(\phi)$  [24–29] as

$$V(\phi) = \frac{1}{8} \left( \frac{\partial W}{\partial \phi} \right)^2 - \frac{1}{3} W^2, \quad (5)$$

hence that first order equations reads

$$\phi' = \frac{1}{2} \frac{\partial W}{\partial \phi}, \quad A' = -\frac{1}{3} W.$$

The SG potential is achieved with the superpotential function by  $W(\phi) = 3bc \sin \left( \sqrt{\frac{2}{3b}} \phi \right)$  [20], which implies on the following solutions

$$\phi(y) = \sqrt{6b} \arctan \left[ \tanh \left( \frac{cy}{6} \right) \right], \quad A(y) = -b \ln(\cosh(cy)). \quad (6)$$

So by substituting Eq. (5) with the superpotential  $W(\phi)$  on the Eq. (5) we obtained the SG potential

$$V(\phi) = \frac{3}{8} bc^2 \left[ 1 - 4b + (1 + 4b) \cos \left( \sqrt{\frac{8}{3b}} \phi \right) \right], \quad (7)$$

where the constants,  $b$  and  $c$ , adjust the  $\phi$  value when  $y \rightarrow \pm\infty$  and control the thickness of the defect, respectively.

The energy density  $\varepsilon(y)$  for de SG model is given by  $\exp(2A(y)) [1/2\phi'^2 + V(\phi)]$ , with the help of equations (6) and (7), it results on the following expression

$$\varepsilon(y) = \frac{3}{2} bc^2 \cosh(cy)^{-2(1+b)} [1 - 2b \sinh(cy)^2]. \quad (8)$$

For the sine-Gordon model, we plot the warpfactor and the energy density in Fig. 1.

### A. Double sine-Gordon brane

Another class of SG potential can provide us two-kink solutions [30–33]. Such potential is named double sine-Gordon because it has a relative minimum at  $\Phi = \pm\pi$  beyond the absolute minimum at  $(0, 2\pi)$  resulting on double bounce solutions to the scalar field. The changing in the original vacua of the SG model give us a new scalar field solution interpolating between the two vacua  $(0$  and  $2\pi)$  with a transient state at  $\pi$  [32–35].

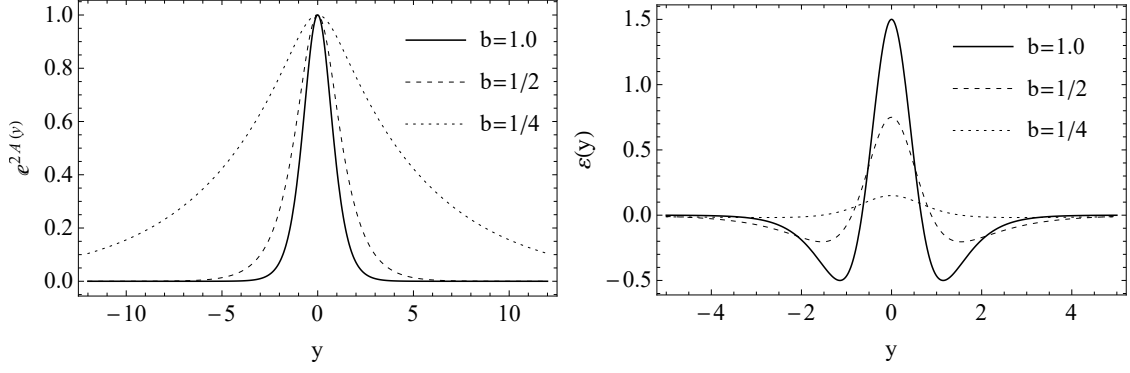


Figure 1: Plots of the warpfactor  $e^{2A(y)}$  (left) and energy density  $\varepsilon(y)$  (right) for some values of  $b$  on the sine-Gordon model ( $c = 1$ ).

Starting from the action (1), we propose the new superpotential with the aim of finding a new solution capable of interpolating both DSG and SG models

$$\mathcal{W}(\Phi) = 4 \cos(\Phi/2) \sqrt{a + 2(1 + \cos(\Phi))} + 2a \ln \left[ 2 \cos(\Phi/2) + \sqrt{a + 2(1 + \cos(\Phi))} \right], \quad (9)$$

that result on the new modified DGS potential

$$\begin{aligned} \mathcal{V}(\Phi, \pi) &= \frac{1}{8} \left( \frac{\partial \mathcal{W}}{\partial \Phi} \right)^2 - \frac{1}{3} \mathcal{W}^2 \\ &= 1 - \cos(2\Phi) + a(1 - \cos(\Phi)) - \frac{5}{4} \left[ 2 \cos(\Phi/2) \sqrt{a + 2(1 + \cos(\Phi))} \right. \\ &\quad \left. + a \ln \left( 2 \cos(\Phi/2) + \sqrt{a + 2(1 + \cos(\Phi))} \right) \right]^2, \end{aligned} \quad (10)$$

We denote by  $\Phi(y)$  the scalar field on the DSG setup obtained numerically from the first-order equation  $\Phi' = \frac{1}{2} \frac{\partial \mathcal{W}}{\partial \Phi}$ . In the Fig. 2 we plot the SG and the DSG potentials with the respective solutions to the scalar field. The minima of the SG potential correspond to the vacua of  $\phi(y)$ , however, on the DSG scenario, there is a local minimum at  $\Phi = \pi$  beyond the minima at  $\Phi = 2\pi$ . The existence of the local minima results on the structure of double bounce.

In fact, is it possible to obtain a single kink solution from the DSG potential. In the figure (3), we have plotted the DSG potential, and the respective scalar field solutions were varying the parameter  $a$ . The structure of the scalar field solution with two bounces transits to a kink-like solution. Such transformation coincides with the vanishing of the transient minimum in the DSG potential at  $\Phi = \pi$ .

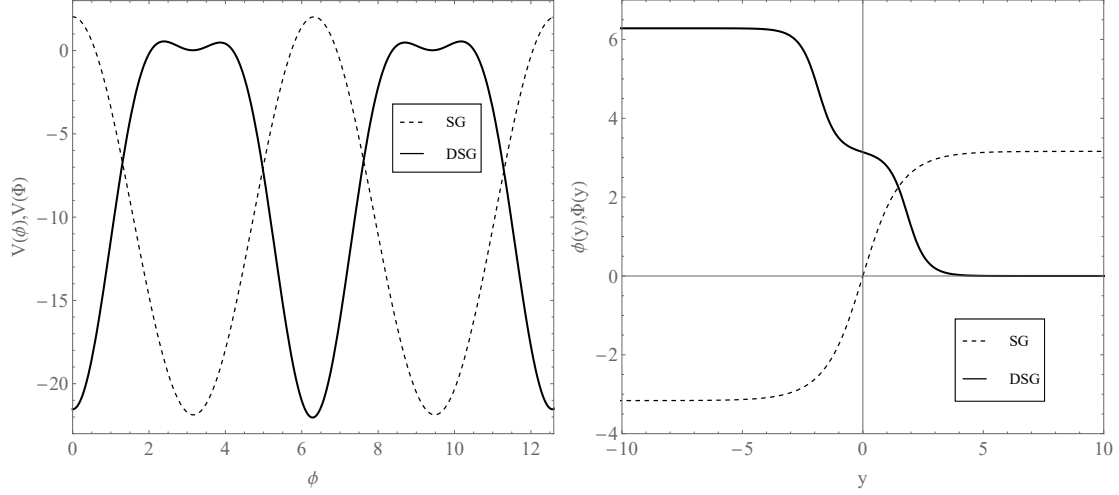


Figure 2: Plots of the potential  $\mathcal{V}(\Phi)$  Eq. (10) and  $V(\phi)$  Eq. (7) (left). Plots of  $\phi(y)$  and  $\Phi(y)$  (right). We have used  $a = 0.02$ ,  $b = 2.7$  and  $c = 1$ .

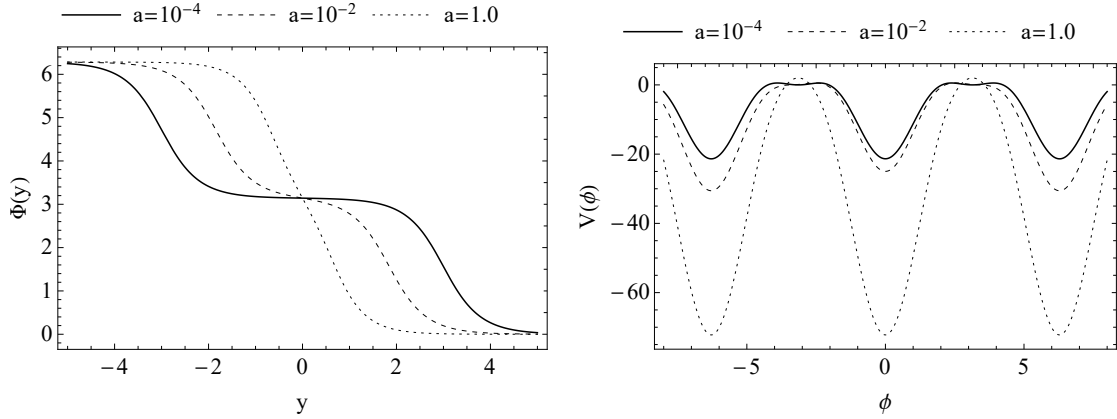


Figure 3: Plots of the fields  $\Phi(y)$  (left panel) and  $V(\phi)$  (right panel) for some  $a$  on the DSG model.

The solution for the warp factor is obtained from equation

$$\mathcal{A}'(y) = -1/3\mathcal{W}(\Phi). \quad (11)$$

We plot the numerical solutions of Eq. (11) in the left panel of Fig. 4, from where we note that the increase of  $a$  narrow the warp-factors.

Finally, the energy-density is given by:

$$\varepsilon(y) = e^{2\mathcal{A}(y)} \left[ \frac{1}{2}\Phi'^2 + \mathcal{V}(\Phi) \right]. \quad (12)$$

this expression is shown in right panel of Fig. 4, where we note the that the increase

of  $a$  confine the energy. The computation of the configurational entropy is based on this energy-density.

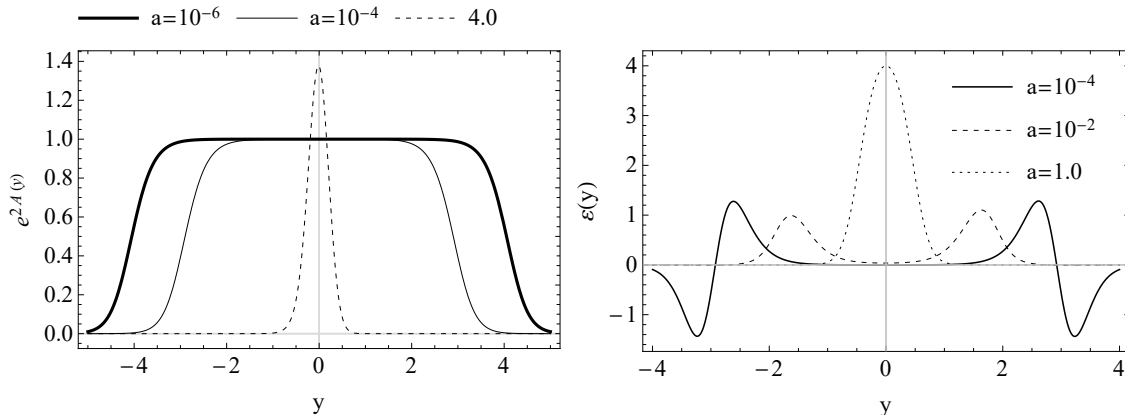


Figure 4: Warpfactors  $e^{2A(y)}$  (left panel) and Energy-density  $\varepsilon(y)$  (right panel) on the DSG model.

Here, we finish the review of the DSG model. In the next section, we will obtain our first result when applying the configurational entropy to the energy-density of the DSG model.

### III. CONFIGURATIONAL ENTROPY

The configurational entropy (CE) is related to the energy of a localized field configuration and can be expressed by the Fourier transform of the energy density [1, 11]. Such quantity was preliminarily considered to study single sine-Gordon braneworlds on the work [16], but the DSG structure was not computed.

To evaluate the CE, we need to define the modal fraction as [1, 36, 38]

$$f(\omega) = \frac{|\mathcal{F}(\omega)|^2}{\int_{-\infty}^{\infty} d\omega |\mathcal{F}(\omega)|^2}, \quad (13)$$

where  $\mathcal{F}(\omega) = -\frac{1}{\sqrt{2\pi}} \int_{-\infty}^{\infty} \varepsilon(y) e^{i\omega y} dy$  is the Fourier transform of the energy density Eq. (12).

Subsequently, we can work with the normalized modal fraction, defined as the ratio of the normalized Fourier transformed function and its maximum value  $\tilde{f}(\omega) = f(\omega)/f_{max}$ . So, localised and continuous function  $\tilde{f}(\omega)$  yields the following definition for the CE:

$$S(\tilde{f}) = - \int_{-\infty}^{\infty} d\omega \tilde{f}(\omega) \ln [\tilde{f}(\omega)]. \quad (14)$$

Firstly we consider the SG model and the respective energy density on the Eq. (8), from where we obtain the Fig. 5. This profile has only a minimum at the origin, which implies no

phase transitions to the scalar fields. This feature was also observed in usual Bloch brane model [12] and the string-cigar brane model [14], where only the single-kink solutions are achieved.

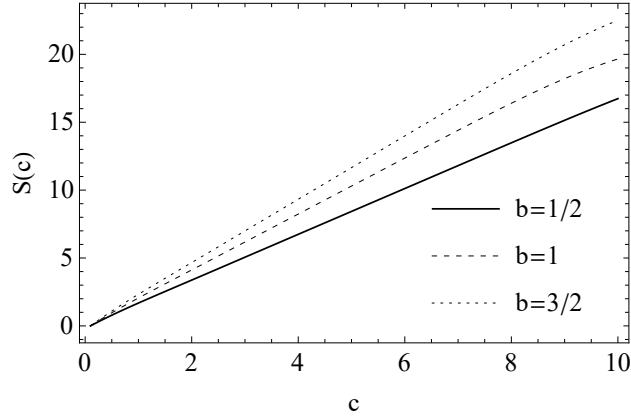


Figure 5: Plots of the CE for SG setup.

Now, we are interested in a more general braneworld generated by the double sine-Gordon potential. As the DSG scenario is capable of creating multi-kink solutions, we expect to achieve a similar behavior to the CE as found in the study of degenerate Bloch branes [12]. In fact, we evaluate the CE numerically and the result is showed in the Fig. 6. Initially,

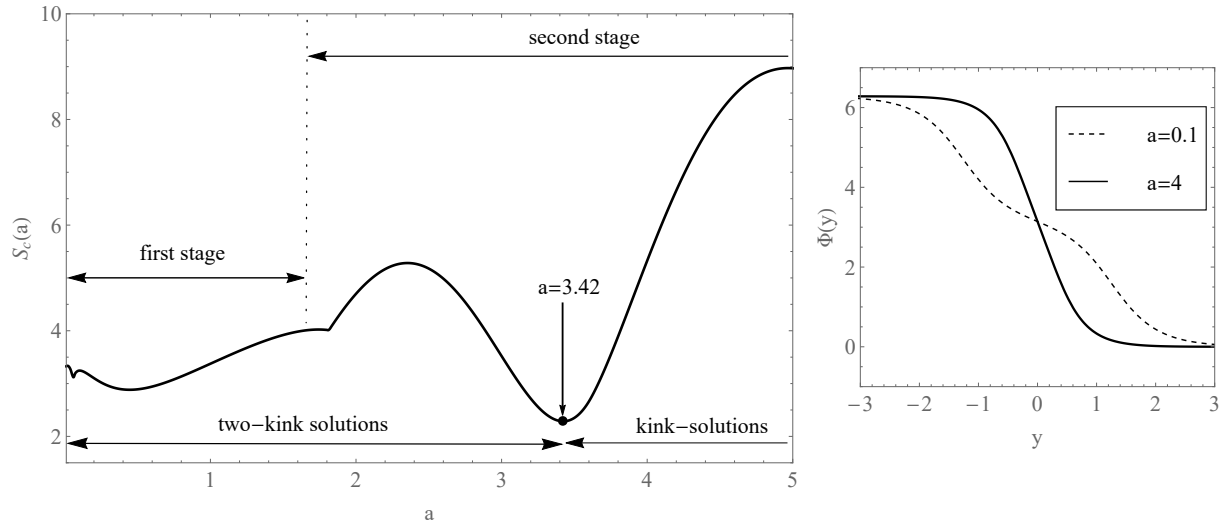


Figure 6: Plots of the CE (left) and the scalar field solution for DSG setup (right).

we observe two sectors with similar behavior, that we named first and second stages. The repeat of the same characteristic with the evolution of the parameter  $a$  is due to the feature

of the DSG potential. In fact, in the first stage, we have the raising of local minima on the DSG potential. Increasing  $a$  the local minima disappear, being replaced by another more prominent local minima on the second stage.

The DSG setup admits the usual kink and also the two-kink solution, as we showed in the Fig. 6. By varying the parameter  $a$ , the scalar field transits smoothly between these two structures with a phase transition localized at the second stage. The changing point from the kink to the two-kink solution occurs at the value of the parameter  $a$  correspondent to the minima CE of the DSG braneworld. A similar result is found in the degenerate Bloch branes models [12].

#### IV. GRAVITY RESONANCES AND CORRECTIONS TO NEWTON'S LAW ON THE DSG MODEL

##### A. Review of gravity localization on the DSG model

This section is organized into three subsections. In the first subsection IV A, we review the gravity localization in the DSG model performed in the Ref. [20]. However, we obtain new results in subsection IV B, where we aim to present the correlation between the gravitons resonance and the CE applied to the DGS model. Moreover, in subsection IV C, we exhibit the new results of the corrections to the short-ranged Newtonian potential due to the massive modes in the DSG model.

We start by describing the conformally flat perturbed metric for our fifth dimension model:

$$ds^2 = e^{2A(y)}(\eta_{\mu\nu} + \epsilon h_{\mu\nu})dx^\mu dx^\nu + dy^2, \quad (15)$$

where  $A(y)$  is the warp factor Eq. (11). The  $\eta_{\mu\nu}$  is the four-dimensional Minkowski metric. The  $h_{\mu\nu} = h_{\mu\nu}(x, y)$  represents the graviton with the axial gauge  $h_{5N} = 0$ . Moreover, imposing the transverse and traceless gauge, the  $\bar{h}_{\mu\nu}$  can be described by the motion equation [24, 39]:

$$\bar{h}_{\mu\nu}'' + 4A'\bar{h}_{\mu\nu}' = e^{-2A}\partial^2\bar{h}_{\mu\nu}', \quad (16)$$

where  $\partial^2$  is the four-dimensional wave operator and the primes denote derivatives with respect to the extra coordinate  $y$ .

In order to obtain a Schrödinger like equation of Eq. (16), we need to transform the extra coordinate into form  $dz = e^{-A(y)}dy$ . Hence the metric of equation (15) become conformally plane  $ds^2 = e^{2A(z)} [(\eta_{\mu\nu} + \epsilon h_{\mu\nu})dx^\mu dx^\nu + dz^2]$ . Further, performing the Kaluza-Klein coordinates decomposition  $\bar{h}_{\mu\nu}(x, z) = e^{ip \cdot x} e^{-\frac{3}{2}A(z)} U_{\mu\nu}(z)$ , we can rewrite the Eq. (16) as a Schrödinger-like equation, which describe the propagation of the gravitational modes into the extra dimension  $z$ .

$$-\frac{d^2 U(z)}{dz^2} + \mathcal{V}(z) U(z) = m^2 U(z), \quad (17)$$

where the quantum-analogue potential reads  $\mathcal{V}(z) = \frac{3}{2}\ddot{A}(z) + \frac{9}{4}\dot{A}^2(z)$ , where the dots denote derivatives with respect to  $z$ .

We plot, in the left panel of figure 7, the potential mentioned above, which assume a volcano-like profile. This potential has two minima and two maxima separated by the flat region around  $z = 0$ . Note that the increase of the  $a$  parameter narrows the width of the well, without reducing the amplitude of the maximum, this result endorses the presence of resonant states [20]. For higher values of  $a$ , the usual volcano-like potential of the SG model is reproduced [20]. It is also important to mention the potential  $\mathcal{V}(z)$  support no tachyonic states [20].

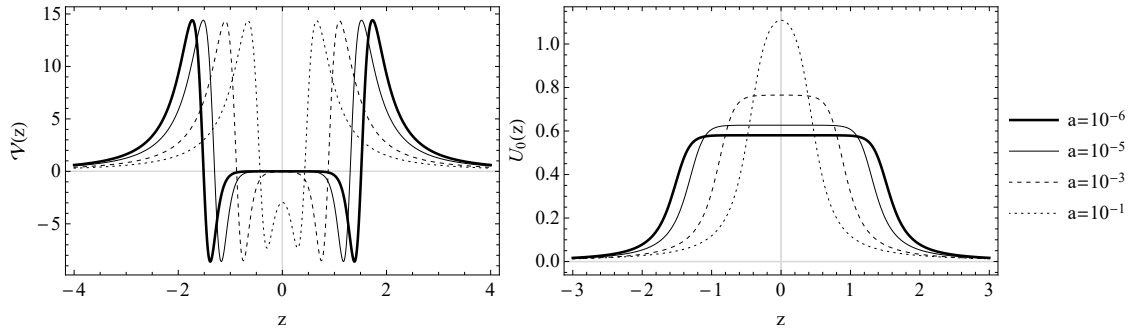


Figure 7: The Schrödinger volcano-like potential for the DSG model (left panel) and the even normalized zero mode of DSG model (right panel). The odd zero mode solutions have not be localized on DSG model.

Moreover, as expected, the equation (17) have an unique localized (normalizable) massless mode solution[20]. This zero mode is responsible for reproduces the four-dimensional gravity. We plot this zero mode in the right panel of figure 7. From where we note, once more time,

that the increase of the  $a$  parameter narrow the width of the zero modes. It is worth highlighting that both even as odd conditions were considered:

$$\begin{aligned} \text{Even condition: } U(z=0) &= cte \quad \text{and} \quad \dot{U}(z=0) = 0 \\ \text{Odd condition: } U(z=0) &= 0 \quad \text{and} \quad \dot{U}(z=0) = cte \end{aligned} \tag{18}$$

However, for the DSG model, only the even solutions was possible to be confined. Initially,  $cte = 1$ , and its value is modified after the wave normalization.

On the other hand, the massive solutions of Eq. (17) are never normalizable, regardless to be an even solution or an odd solution. However, its modes can exhibit resonant states and also can perform corrections to the four-dimensional Newtonian potential. These aspects will be discussed in the next subsection.

## B. Resonances on DSG model

With the 3-brane placed at origin  $z = 0$ , we can compute the coupling of the massive modes with the matter on the brane by solving the Schrödinger-like equation (17). Once that the volcano-like potential  $\mathcal{V}(z)$  represents only a small perturbation, we have the condition the resonant mode should appear inside the well  $m^2 \leq \mathcal{V}_{max}$ . On the other hand, the massive solutions already acquire a plane wave profile after the barrier, when  $m^2 > \mathcal{V}_{max}$ .

The so-called “resonant modes” are wavefunctions which  $U(0)$  own large amplitudes inside the brane (in comparison with its values far away from the brane). In order to find these resonant modes, we adopt the well-known relative probability method  $N(m)$  [40–44] given by

$$N(m) = \frac{\int_{-z_b}^{+z_b} |U_m(z)|^2 dz}{\int_{-z_{max}}^{+z_{max}} |U_m(z)|^2 dz} \tag{19}$$

where  $z_{max}$  denote the maximum box interval for  $z$ , while the narrow interval is given by  $z_b = 0.1z_{max}$  [42].

The function  $N(m)$  useful in the search for resonant modes. The term  $\int_{-z_b}^{+z_b} |U_m(z)|^2 dz$  in Eq. (19) express the probability for finding the resonant modes into a narrow interval  $-z_b < z < z_b$ . It worth to say the choose of the integration range  $z_b = 0.1z_{max}$  do not interferes on the masses of possible existing resonances [45].

We apply the relative probability method  $N(m)$  from Eq. (19) to the DSG model for some values of  $a$  parameter. The Fig. 8 and Fig. 9 was obtained for the even and odd gravity

solutions, respectively. In each figure are embedded a table with the value of resonant mass  $m_*$ , the full width at half maximum  $\Gamma$  and the resonant lifetime  $\tau \approx \Gamma^{-1}$ . For smaller  $a$ , the double peaks are subscribed by (1) and (2) below the  $a$  values.

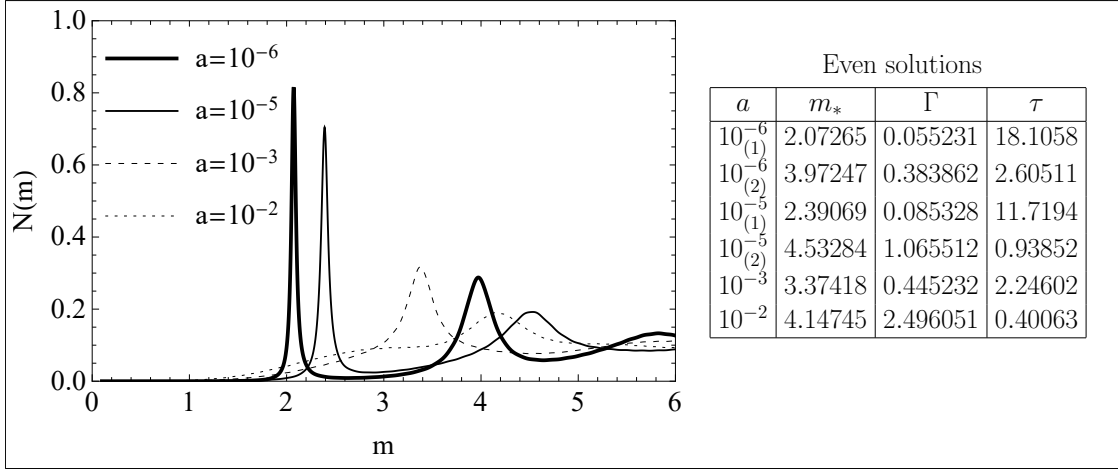


Figure 8:  $N(m)$  method for gravity even solutions on DSG model. The  $m_*$  is the resonant mass,  $\Gamma$  is the the full width at half maximum and  $\tau$  the lifetime. The (1) and (2) labels the double peaks.

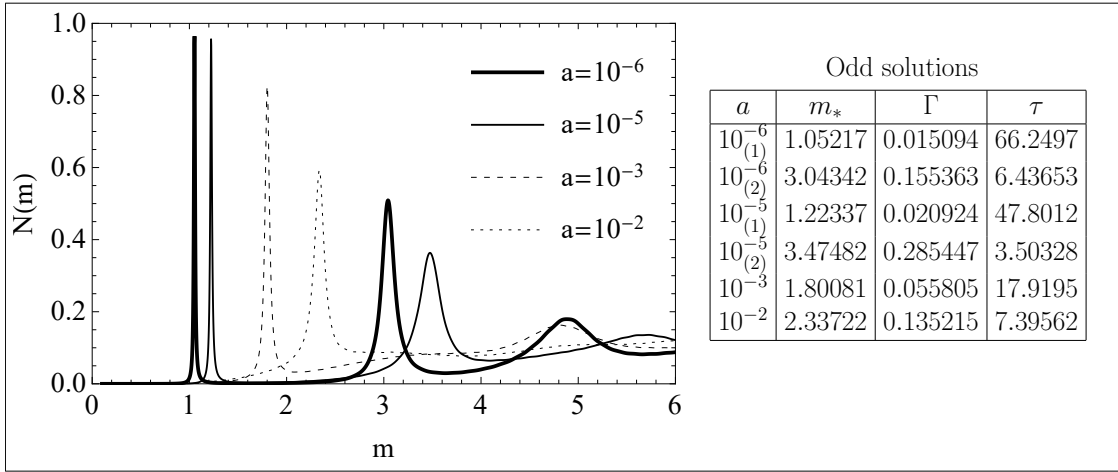


Figure 9:  $N(m)$  method for gravity odd solutions on DSG model. The  $m_*$  is the resonant mass,  $\Gamma$  is the the full width at half maximum and  $\tau$  the lifetime. The (1) and (2) labels the double peaks.

From both figures 8 and 9 we see that  $a = 10^{-6}$  and  $a = 10^{-5}$  own double peaks. By considering only the first peaks, we note that smaller  $a$  have higher peaks, narrower  $\Gamma$  and longer lifetimes  $\tau$ . Longer lifetimes implies in more stable modes. In different circumstances, for larger  $a$  the peaks vanish. Roughly when  $a > 10^{-1}$ , there are no more resonant modes

because the peaks acquire the plane wave profile. This result corroborates the absence of resonant modes on single sine-Gordon models. Additionally, the even solutions have peaks placed at larger mass positions and have shorter lifetimes, if compared to the odd solutions.

Now, after proceeding the analysis of the massive spectra we conclude there is no strong link between the resonance structures and respective lifetimes with the CE. The presence of resonances for odd or even solution is limited for a very narrow interval ( $a < 10^{-1}$ ) of the parameter that controls the brane thickness. Observing the structure of the volcano potential, we note that this is a region where the maxima of the potential are as far apart as possible. Concerning the entropic measure, it corresponds only to the region at the beginning of the first stage interval, inside the two-kink solutions. However, the point where the phase transitions occur (CE minimum) does not present any correlation with the resonant modes.

### C. Correction on Newton's potential from the DSG model

One of the well-known approaches to studying the corrections in Newton's law is through a Yukawa type interaction between two point masses  $M_1$  and  $M_2$  separated by the distance  $x$  in four-dimensions [46–49].

$$V(x) = -G_N \frac{M_1 M_2}{x} [1 + \Delta(x)], \quad \Delta(x) = \alpha e^{-\frac{x}{\lambda}} \quad (20)$$

the  $\alpha$  and  $\lambda$  are adjustable parameters. The Ref. [46] present a review of these corrections in some theoretical models, while the [47] test the experimental valid of these corrections.

In the braneworlds context, each massive model contributes to the corrections to Newton's potential [48–50]. The term  $\lambda = 1/m$  and the amplitude term reads  $\alpha(m) = e^{-\frac{3}{2}A(z)} \hat{U}(z)$  [48–50], being  $\hat{U}(z)$  the normalized eigenfunction from Eq (17). The  $\alpha(m)$  should be applied the extra-dimensional position where the brane is placed  $z = 0$  [49]. So, note that the corrections are decreases exponentially both with the increasing of the mass and the position. Therefore, for a continuous mass interval, we can express Newton's corrections due to the massive modes in a five-dimensional model as an integral over the massive modes

$$\Delta(x) \propto \int_{m_1}^{\infty} \left[ e^{-\frac{3}{2}A(z)} \hat{U}(z) \right]_{z=0}^2 e^{-m_n x} dm \quad (21)$$

where  $\hat{U}(z)$  is the normalized eigenfunction from Eq (17) and  $m_1$  the mass of first excited state.

For the DSG model, we solve numerically the equation (17), considering only the even-solutions, since that the odd-solutions are null at  $z = 0$  and do not contribute to the corrections. We use the mass interval  $0.1 \leq m \leq 10$  and the DSG parameters  $a = 10^{-6}$ ,  $a = 10^{-2}$ ,  $a = 3.5$ , additionally the solutions of the SG model. From these massive eigenfunctions, the plot in Fig. 10 represent the integrand  $\Theta(m, x, a)$  of  $\Delta(x)$  equation Eq. (21). From where we note, when  $x = 0$ , that the profile of  $\Theta(m, x, a)$  shares some similarity with the even-solutions resonances for  $a = 10^{-6}$  and  $a = 10^{-2}$  in Fig. 8, decreasing as  $x$  grows. Note that the integrand of  $a = 3.5$  (DSG model with single kink) and the integrand of the SG model are similar. Moreover, for smaller values of  $a$ , we note that the multi-resonance states perform more intense corrections at the origin. Increasing the  $a$  the corrections are suppressed, converging the corrections of DSG model into SG.

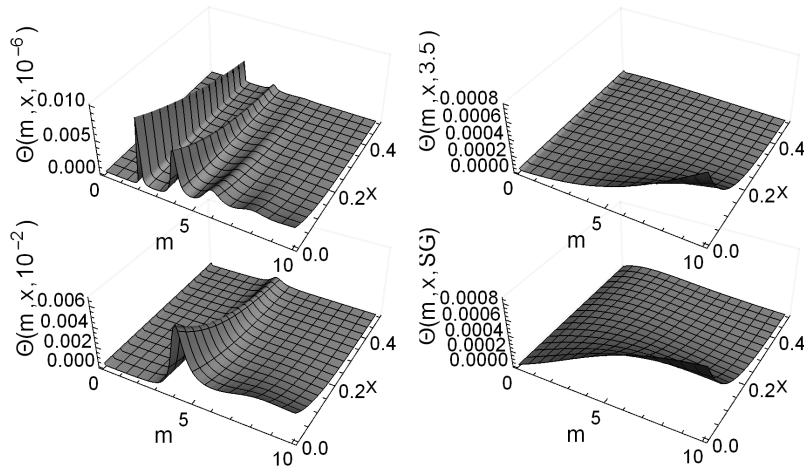


Figure 10: The  $\Theta(m, x, a)$  integrand of the  $\Delta(x)$  for  $a = 10^{-6}$  (top-left panel),  $a = 10^{-2}$  (bottom-left panel),  $a = 3.5$  (top-right) and for the SG model (bottom-right).

The plot of the  $\Delta(x)$  corrections to Newton's potential are present in Fig. 11. From where we note that the increase of  $a$  parameter decreases the shape of the corrections. The profiles for  $a = 10^{-6}$  and  $a = 10^{-2}$  have similar results, the same occurs for  $a = 3.5$  and the SG corrections.

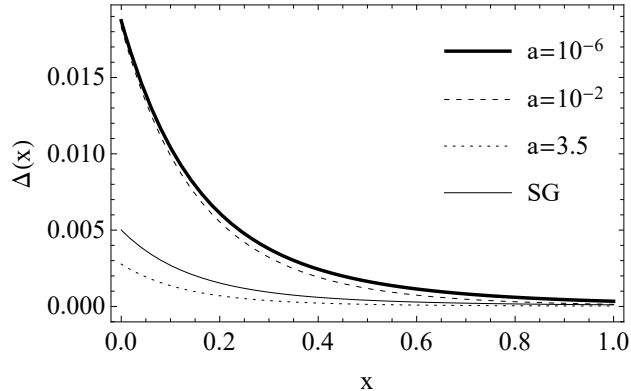


Figure 11:  $\Delta(x)$  corrections to Newton's potential for some DSG model parameters and the SG model.

## V. SUMMARY

In this work we compute the configurational entropy (CE) and the corrections to Newton's Law in five dimensional sine-Gordon brane models, focusing on the double sine-Gordon model (DSG). We conclude that the minimums of CE endorse the phase transitions from kink to multi-kinks. For the DSG this phase occurs when  $a \sim 3.42$ . Moreover, we compute the graviton resonances in the DSG model, which occur only in the first region (double-kink solution) where CE have lower values. However, the point where the phase transitions occur (CE minimum) does not present any correlation with the resonant modes. Finally, we have performed the corrections to Newton's potential in DSG varying the  $a$  parameter. We note that the corrections to Newton's potential share some similarities with the resonant profiles. We conclude that smaller  $a$  exhibit longer life-time and multi resonances states, which have more significant contributions to the corrections. For the greater  $a$  parameter, the resonances vanish, and the single kink profile is achieved, taking the DSG model into a similar form of the SG model.

## Acknowledgments

The authors thank the Fundação Cearense de apoio ao Desenvolvimento Científico e Tecnológico (FUNCAP), the Coordenação de Aperfeiçoamento de Pessoal de Nível Superior (CAPES), and the Conselho Nacional de Desenvolvimento Científico e Tecnológico (CNPq)

for financial support.

---

- [1] M. Gleiser and N. Stamatopoulos, *Phys. Lett. B* **713**, 304 (2012).
- [2] C. E. Shannon, *The Bell System Technical J.* **27**, 379 (1948).
- [3] M. Gleiser and D. Sowinski, *Phys. Lett. B* **727**, 272 (2013)
- [4] M. Gleiser and N. Stamatopoulos, *Phys. Rev. D* **86**, 045004 (2012).
- [5] M. Gleiser and N. Jiang, *Phys. Rev. D* **92**, no. 4, 044046 (2015)
- [6] A. E. Bernardini and R. da Rocha, *Phys. Lett. B* **762**, 107 (2016)
- [7] N. R. F. Braga and R. da Rocha, *Phys. Lett. B* **776**, 78 (2018)
- [8] A. Goncalves da Silva and R. da Rocha, *Phys. Lett. B* **774**, 98 (2017)
- [9] R. Casadio and R. da Rocha, *Phys. Lett. B* **763**, 434 (2016)
- [10] M. Gleiser and N. Jiang, *Int. J. Theor. Phys.* **57**, no. 6, 1691 (2018).
- [11] R. A. C. Correa, P. H. R. S. Moraes, A. de Souza Dutra, and R. da Rocha, *Phys. Rev. D* **92**, 126005 (2015); R. A. C. Correa and P. H. R. S. Moraes, *Eur. Phys. J. C* **76**, 100 (2016).
- [12] W. T. Cruz, D. M. Dantas, R. A. C. Correa and C. A. S. Almeida, *Phys. Lett. B* **772**, 592 (2017)
- [13] R. A. C. Correa, D. M. Dantas, P. H. R. S. Moraes, A. de Souza Dutra, and C. A. S. Almeida, *Annalen der Physik.* **530**, 1700188 (2018)
- [14] R. A. C. Correa, D. M. Dantas, C. A. S. Almeida and R. da Rocha, *Phys. Lett. B* **755**, 358 (2016).
- [15] M. Chinaglia, W. T. Cruz, R. A. C. Correa, W. de Paula and P. H. R. S. Moraes, *Phys. Lett. B* **779**, 16 (2018)
- [16] R. A. C. Correa and R. da Rocha, *Eur. Phys. J. C* **75**, 522 (2015).
- [17] G. P. de Brito, R. A. C. Correa and A. de Souza Dutra, *Phys. Rev. D* **89**, no. 6, 065039 (2014).
- [18] O.M. Braun, T. Dauxois, M.V. Paliy, and M. Peyrard. *Phys. Rev. Lett.* **78**, 1295 (1997).
- [19] A.V. Ustinov, B.A. Malomed, and S. Sakai. *Phys. Rev. B* **57**, 11691 (1998).
- [20] W. T. Cruz, R. V. Maluf, L. J. S. Sousa and C. A. S. Almeida, *Annals Phys.* **364**, 25 (2016).
- [21] W. T. Cruz, R. V. Maluf, D. M. Dantas and C. A. S. Almeida, *Annals Phys.* **375**, 49 (2016)
- [22] C. Csaki, J. Erlich, T. J. Hollowood and Y. Shirman, *Phys. Rev. Lett.* **84** 5932 (2000).
- [23] G. Dvali, G. Gabadadze, M. Porrati, *Phys. Lett. B* **484** (2000) 112.

- [24] O. Dewolfe, D.Z. Freedman, S.S. Gubser and A. Karch, Phys. Rev. D 62, 046008 (2000).
- [25] D. Bazeia, M. J. dos Santos and R.F. Ribeiro, Phys. Lett. A208, 84 (1995).
- [26] D. Bazeia and F.A. Brito, Phys. Rev. Lett. 84, 1094 (2000).
- [27] M.A. Shifman and M.B. Voloshin, Phys. Rev. D 57, 2590 (1998).
- [28] A. Alonso Izquierdo, M.A. Gonzalez Lion and J. Mateos Guilarte, Phys. Rev. D 65, 085012 (2002).
- [29] M. Cvetič, S. Griffies, Nucl. Phys. B381, 301 (1992).
- [30] D. Bazeia, J. Menezes, and R. Menezes, Phys. Rev. Lett 91, 241601 (2003).
- [31] C. A. Condat, R. A. Guyer, and M. D. Miller, Phys. Rev. B 27, 474 (1983).
- [32] C. A. Popov, Wave Motion 42, 309 (2005).
- [33] W. Abdul-Majid, Phys. Lett. A 350, 367 (2006).
- [34] N. Riazi and A.R. Gharaati, Int. J. Theor. Phys. 37, 1081 (1998).
- [35] G. Mussardo, V. Riva, and G. Sotkov, Nucl. Phys. B 687, 189 (2004).
- [36] M. Gleiser, D. Sowinski, Phys. Lett. B **727**, 272 (2013).
- [37] M. Gleiser, N. Graham, Phys. Rev. D **89**, 083502 (2014).
- [38] M. Gleiser and N. Stamatopoulos, Phys. Rev. D **86**, 045004 (2012).
- [39] M. Gremm, Phys. Lett. B478, 434 (2000).
- [40] Yu-Xiao Liu, Hai-Tao Li, Zhen-Hua Zhao, Jing-Xin Li, Ji-Rong Ren, JHEP 0910, 091 (2009).
- [41] Yu-Xiao Liu, Chun-E Fu, Heng Guo, Hai-Tao Li, Phys. Rev. D85, 084023 (2012).
- [42] Yu-Xiao Liu, Jie Yang, Zhen-Hua Zhao, Chun-E Fu, Yi-Shi Duan, Phys. Rev. D80, 065019 (2009).
- [43] Yu-Xiao Liu, Chun-E Fu, Li Zhao, Yi-Shi Duan, Phys. Rev. D80, 065020 (2009).
- [44] Hai-Tao Li, Yu-Xiao Liu, Zhen-Hua Zhao, Heng Guo, Phys. Rev. D83, 045006 (2011).
- [45] W. T. Cruz, L. J. S. Sousa, R. V. Maluf and C. A. S. Almeida, Phys. Lett. B **730**, 314 (2014).
- [46] J. Murata and S. Tanaka, Class. Quant. Grav. **32**, no. 3, 033001 (2015)
- [47] D. J. Kapner, T. S. Cook, E. G. Adelberger, J. H. Gundlach, B. R. Heckel, C. D. Hoyle and H. E. Swanson, Phys. Rev. Lett. **98**, 021101 (2007)
- [48] Maxim Gabella. The Randall-Sundrum model. <http://www-thphys.physics.ox.ac.uk/people/MaximeGabella/rs.pdf>. 2006.
- [49] C. Csaki, J. Erlich, T. J. Hollowood and Y. Shirman, Nucl. Phys. B **581**, 309 (2000)
- [50] L. Randall, R. Sundrum, Phys. Rev. Lett. 83, 3370 (1999); *ibid* 83, 4690 (1999).